HSynthesis and Characterization of a Luminescent Cyclic Poly(ethylene oxide)-Polypyridyl Ruthenium Complex

M. Ali Aboudzadeh,[a,b$] Vanessa Rodríguez-Fanjul,[c] Alessio Terenzi,[a#] Estibaliz Gónzalez de San Román,[d] José I. Miranda,[e] Ana M. Pizarro,[c,f*] Luca Salassa,[a,g,h*] and Fabienne Barroso-Bujans[a,b,h*]

[a]*Donostia International Physics Center (DIPC), Paseo Manuel Lardizabal 4, 20018 Donostia−San Sebastian, Spain*

[b]*Materials Physics Center, CSIC-UPV/EHU, Paseo Manuel Lardizabal 5, 20018 Donostia−San Sebastian, Spain*

[c]*IMDEA Nanociencia, Faraday 9, 28049 Madrid, Spain*

[d]*POLYMAT, University of the Basque Country UPV/EHU, Joxe Mari Korta Center, Avda. Tolosa 72, 20018 Donostia−San Sebastian, Spain*

[e]*SGIKer, NMR Service, University of the Basque Country UPV/EHU, Joxe Mari Korta R&D Ctr, Avda. Tolosa-72,* Donostia−*San Sebastian 20018, Spain*

[f]*Unidad Asociada de Nanobiotecnología CNB-CSIC-IMDEA, 28049 Madrid, Spain*

[g]*Polimero eta Material Aurreratuak: Fisika, Kimika eta Teknologia, Kimika Fakultatea, Euskal Herriko Unibertsitatea UPV/EHU, Paseo Manuel de Lardizabal 3, Donostia−San Sebastian, 20018, Spain*

[h]*IKERBASQUE - Basque Foundation for Science, María Díaz de Haro 3, E-48013 Bilbao, Spain*

*E-mail: ana.pizarro@imdea.org (A. Pizarro), lsalassa@dipc.org (L. Salassa) and fbarroso@dipc.org (F. Barroso-Bujans)

Abstract

We report the synthesis of a macrocyclic poly(ethylene oxide) (PEO) connected by one $[Ru(bpy)_3]^{2+}$ unit (where bpy = 2,2'-bipyridine), a photoactive metal complex that provides photosensitivity and potential biomedical applications to this polymer structure. The PEO chain provides biocompatibility, water solubility, and topological play. The macrocycles were successfully synthesized by copper-free click cycloaddition between a bifunctional dibenzocyclooctyne (DBCO)-PEO precursor and 4,4'-diazido-2,2'-bipyridine, followed by complexation with $[Ru(bpy)_2Cl_2]$. The cyclic product accumulated efficiently in MCF7 cancer cells and exhibited a longer fluorescence lifetime than its linear analog, likely due to differences in the accessibility of the ligand-centered/intra-ligand states of Ru polypyridyls in both topologies.

for Table of Contents use only

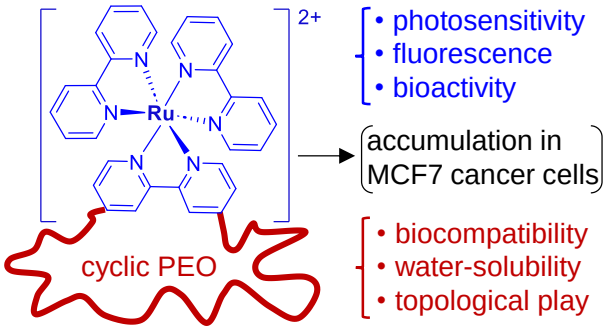

Cyclic polymers have no chain ends resulting in unique physical and chemical properties that distinguish them from linear polymers. Due to topological restrictions, cyclic polymers have shown differentiated chain mobility with respect to linear chains.[1-3] In "hard" nanopores, cyclic poly(ethylene oxide) (PEO) [or poly(ethylene glycol) (PEG)] of

medium-low molecular weight (MW) has shown enormous differences in the pore diffusion respect to linear analogues. For instance, cyclic PEO of 2-20 kDa[4] and smaller crown ether analogues[5-6] showed significantly slower intercalation rates into graphite oxide (a 2D material with an interlayer distance of 5.6 Å) compared to their linear counterparts. Similarly, the intercalation of cyclic PEO of 1-10 kDa into metal-organic frameworks (formed by 1D nano-channels with an aperture of d = 5.7 Å along the c-axis)[7] occurred much slower, if some, compared to their linear analogues, demonstrating that topology is an important factor that influences polymer transport. This effect has important implications in the pharmaceutical use of cyclic polymers. The lifetime of a molecule in the circulatory system is limited by the efficient filtration of foreign materials and waste by the semipermeable nanoporous barrier in the kidneys.[2] Linear chains can easily reptate through the nanopore, whereas in cyclic polymers, two segments of the chain backbone must diffuse simultaneously. This slows down or even prevents the penetration of the chain into the pore. *In vivo* studies in mice demonstrated that cyclic PEGylated poly(ε-caprolactone) comb polymer with MW above the renal filtration threshold (>50 kDa) is retained in blood plasma longer than its linear analog,[8] illustrating the potential applications of cyclic polymers as drug carriers or imaging agents. Below the renal filtration threshold, both, cyclic and linear polymers of 32 kDa, were rapidly eliminated, but the more compact nature of the cyclic structure caused a faster elimination respect to the linear analog. Moreover, cyclic PEGylated poly(acrylic acid) comb polymers with MW above the renal filtration threshold showed the capacity to accumulate preferentially in target tumor cells by means of the enhanced permeability and retention (EPR) effect,[9] demonstrating how this class of materials may prove useful for biomedical applications.

Covalent anchoring of photoactive metal complexes onto biocompatible polymers such as PEG is currently attracting much interest for application in medicine (e.g., photodynamic therapy).[10-11] Polymer loading of metal-based agents can in principle afford innovative materials with better pharmacokinetics, reduced systemic toxicity, enhanced cell uptake, and even improved photophysical features.[12] The incorporation of metallo-supramolecular interactions in polymeric systems has been widely used to generate specific nanostructures such as stars, dendrimers, multiblock copolymers, crosslinked networks and cyclic brush polymers.[13-16] These interactions can be based in the formation of only one metal-ligand complex (*eg.* to form copolymers) or multiple-metal-ligand complexes (*eg.* to form brush copolymers). We were intrigued by the prospect of generating cyclic polymeric chains connected by one ruthenium polypyridyl complex, a structure that combines the benefits of both, the circular polymeric structure and the presence of a metal center. Derivatives of the prototypical $[Ru(bpy)_3]^{2+}$ (where bpy = 2,2'-bipyridine) have found numerous applications because of their unique photophysics and photochemistry, including in energy conversion,[17] photoredox catalysis,[18] photochemotherapy,[19-20] and imaging.[21]

Herein, we present the first example of a cyclic macromolecule composed by a PEO chain with a circular structure connected by one $[Ru(bpy)_3]^{2+}$ unit (CPEO-[Ru]) as a proof of concept of a photoactive cyclic PEO. To optimize the synthesis method of these structures we focused on the study of low MW compounds with molecular masses well below the renal filtration threshold. The photophysical behavior of the generated Ru-containing polymer was studied in comparison to its linear LPEO-[Ru] analog by means of UV-Vis and fluorescence spectroscopy, together with their capacity to enter and accumulate in cancer cells in flow cytometry experiments. This work is the first step toward the design

of new cyclic metallo-polymers that may have advantageous tissue penetration properties for use in medicine.

The synthetic route to CPEO-[Ru] and its analogous linear LPEO-[Ru] are depicted in Figures 1a and 1b. Copper-free click chemistry reaction of 4,4'-diazido-2,2'-bipyridine and DBCO-functionalized PEO was implemented to generate both structures (FTIR and NMR spectra shown in Figures S1 and S2). The cyclic CPEO-bpy was produced by means of a bimolecular homodifunctional cyclization approach[22] using bifunctional DBCO-PEO-DPCO of M_n = 2 kg/mol. LPEO-bpy was generated by using monofunctional DBCO-PEO-OMe of M_n = 1 kg/mol. Gel permeation chromatography (GPC) data of CPEO-bpy showed the expected increase of peak retention time originated from chain compaction whereas that of LPEO-bpy displayed a decrease of the retention time due to chain elongation (Figure 2a). The formation of triazole rings was confirmed in the ^{1}H NMR experiments by changes in the 6.5-9.0 ppm region (aromatic signals) and the appearance of two sets of signals c,c' in the 4.3-6.5 ppm region (Figure 2b). These resonances are attributed to the formation of two isomers, the 1,5- and 1,4-substituted triazole rings (Figure 2c). The c,c' signals are very sensitive to any chemical transformation in the DBCO unit, as observed by a notable shift from the unreacted DBCO-PEO precursors (c, c' = 5.15 and 3.65 ppm, Figures S3-S5) to PEO-bpy compounds (c, c' = 6.32 and 4.51 ppm; 5.60 and 5.04 ppm, Figure 2b and Figures S7-S8). In an attempt to quantify the cyclic purity of CPEO-bpy, GPC data of Figure 2a was deconvoluted in two peaks assuming that unreacted PEO chains appears at lower retention times (Figure S9a). The peak area of this possible linear impurity was 14 % of the total area. However, it is likely that this value is much lower since there is no spectroscopic evidence (within the limits of detection) of the presence of unreacted DBCO units in the ^{1}H NMR spectrum of CPEO-bpy, by using the signal "c"

of DBCO-PEO-DBCO precursor as indicator (Figure S9b), nor the presence of unreacted DBCO-PEO-DBCO in the MALDI-ToF mass spectrum of CPEO-bpy.

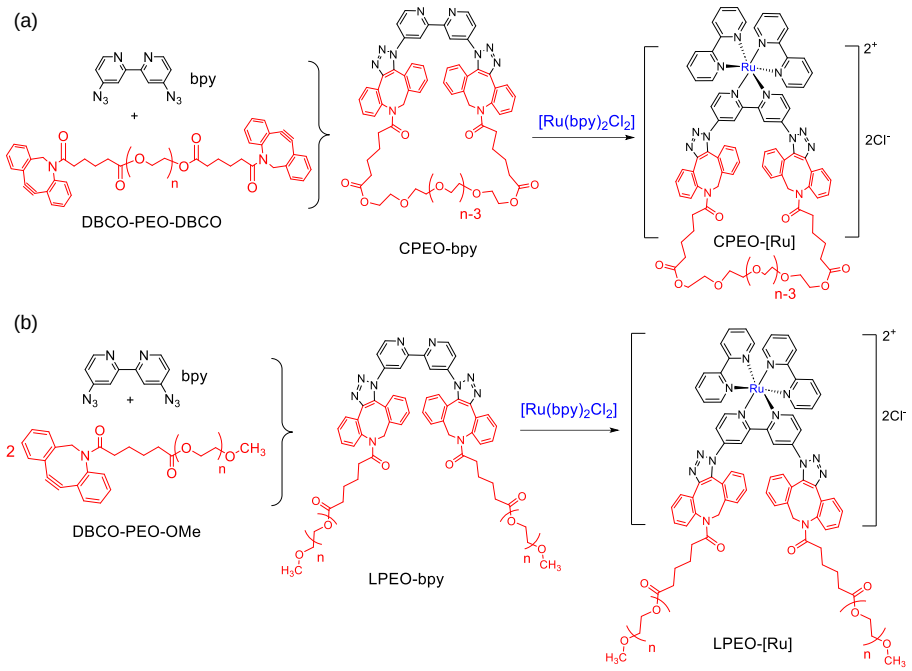

Figure 1. Scheme of synthesis of (a) CPEO-[Ru] and (b) LPEO-[Ru].

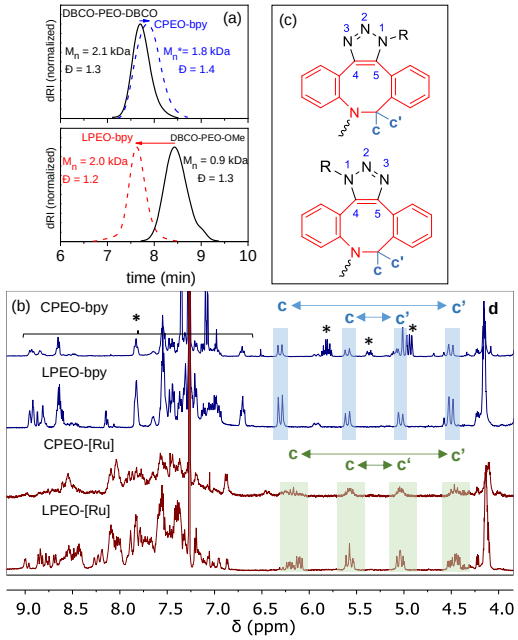

Figure 2. (a) GPC data (DMF + 0.1 % LiBr) of CPEO-bpy, LPEO-bpy and their PEO precursors. M_n*: underestimated molecular weight (see SI). (b) ^{1}H NMR spectra (in $CDCl_3$) of CPEO-bpy and LPEO-bpy exhibiting the appearance of two set of signals c,c'

upon triazole formation. (*) Aromatic signals, see HSQC in Figure S7. Signal d, OCO$\underline{CH_2}$ of PEO chain, see Figure S3. ^{1}H NMR spectra (in $CDCl_3$) of CPEO-[Ru] and LPEO-[Ru] exhibiting a change in the multiplicity of c,c' signals upon Ru-$(bpy)_2$ incorporation. (c) Isomers.

Both, CPEO-bpy and LPEO-bpy were reacted with $[Ru(bpy)_2Cl_2]$ to generate the Ru-complexes of PEO. The products were purified in a preparative GPC, allowing us to remove undesired byproducts and to split the main product in two fractions of different molecular weights (f1 and f2, Table S3) which guaranteed the use of samples with the highest possible topological purity in further experiments. ^{1}H NMR data of Ru-complexes (Figure 2b and Figures S10-S11) exhibited a notable change in the aromatic region compared to Ru-free compounds as well as a change in the multiplicity of c,c' signals as a result of the conformational blocking of DBCO groups upon the incorporation of the Ru-$(bpy)_2$ unit into the polymer.

MALDI-ToF MS experiments confirmed the incorporation of Ru-$(bpy)_2$ moieties into the PEO-bpy chains by a notable change in the isotopic distribution from Ru-free to Ru-coordinated species (Figures 3 and 4). Ru-free compounds, CPEO-bpy and LPEO-bpy, exhibit a distribution of peaks separated by m/z 44, the mass of an ethylene oxide unit. The observed mass (m_{obs}) at the peak position, where the calculated monoisotopic mass (m_{theo}) of Na^+ cationized species is expected ($[M+Na]^+$), matches with both structures, CPEO-bpy and LPEO-bpy, thus confirming their synthesis. Ru is composed of seven stable isotopes, which combined with the isotopes of other elements in the polymer, results in complex mass spectra with a specific peak pattern. Identification of Ru-complexes can be difficult since these species can react during the MALDI experiment and cause ion loss (such as Cl^-), addition of ligands, matrix molecules or solvents.[23-24] In

our data, Ru-containing ions were identified as those generated by losing two bpy ligands and a Cl^- anion $[M\text{-}2bpyCl]^+$. Species formed by the addition of Na^+ were not detected. Addition of K^+ conducted to same results (data not shown) corroborating previous assignment. In CPEO-[Ru], we observed a second specimen overlapped with that identified as $[M\text{-}2bpyCl]^+$, which could be a neutral species formed by the $[CPEO\text{-}Ru]Cl_2$ salt ([M] in Figures 3b and 3c). The neutral salt was not detected in LPEO-[Ru], allowing a clearer identification of $[M\text{-}2bpyCl]^+$ specimens. Other species with lower peak intensities were also observed in LPEO-[Ru] which could be attributed to the loss of only one bpy ligand resulting in the neutral species [M-bpy] (Figure 4b). Theoretical isotopic patterns of CPEO-[Ru] and LPEO-[Ru] specimens are given in Figures S12-S14, which compare very well with the experimental data.

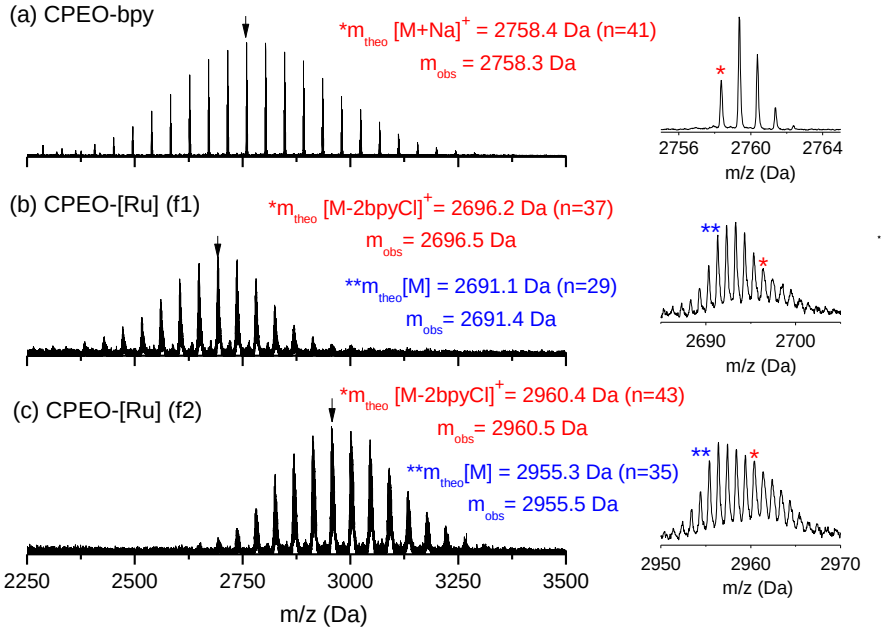

Figure 3. MALDI-ToF MS of (a) CPEO-bpy and (b, c) CPEO-[Ru] (f1, f2). M represents the analyte. Right figures: Isotopic distribution of the peaks indicated by arrows. In (a) the cationized species are formed by the addition of Na^+. In (b, c) two specimens coexist, a cation formed by the loss of two bpy ligands and a chloride anion, $[M\text{-}2bpyCl]^+$, and the

neutral species [M]. (*) and (**) indicates the calculated monoisotopic mass (m_{theo}) for each species (Figures S12 and S14). The observed mass (m_{obs}) corresponds to the peak mass at the peak position where the monoisotopic peak is expected to appear. "n" indicates the number of ethylene oxide units.

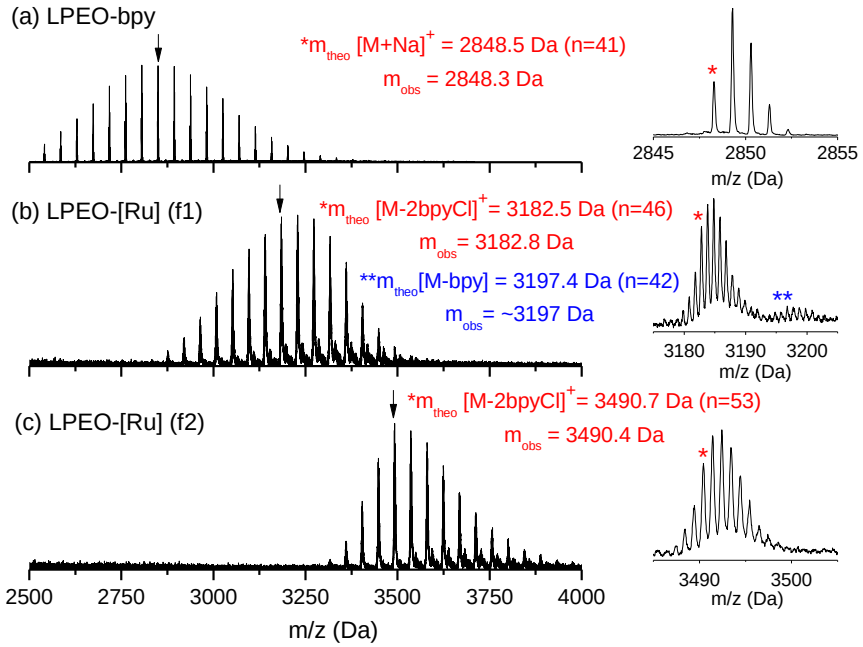

Figure 4. MALDI-ToF MS of (a) LPEO-bpy and (b, c) LPEO-[Ru] (f1, f2). M represents the analyte. Right figures: Isotopic distribution of the peaks indicated by arrows. In (a) the cationized species are formed by the addition of Na^+. In (b, c) a cation is formed by the loss of two bpy ligands and a chloride anion, $[M-2bpyCl]^+$. (*) indicates the calculated monoisotopic mass (m_{theo}) (Figure S13). (**) shows a secondary neutral specimen that could be attributed to the loss of one bpy ligand, [M-bpy] (Figure S14). The observed mass (m_{obs}) corresponds to the peak mass at the peak position where the monoisotopic peak is expected to appear. "n" indicates the number of ethylene oxide units.

Absorption and emission features of CPEO-[Ru] and LPEO-[Ru] were investigated in aqueous solution (Figure 5). The absorption spectrum of the cyclic derivative resembled the characteristic profile of the prototypical complex $[Ru(bpy)_3]Cl_2$,[25] displaying ligand-centered bands at high energies and, prevalently, a metal-to-ligand charge transfer (MLCT) band at 450 nm. In the LPEO-[Ru] case, a broader absorption was visible between 350–500 nm, with maxima at 336, 424, and 489 nm. This feature can be ascribed to the co-existence of intense MLCT and ligand-centered/intra-ligand (LC/IL) transitions in this wavelength range.[26] DFT and TD-DFT calculations performed on a model structure of the Ru polypyridyl core show that indeed MLCT and LC/IL singlet transitions are present in the lower-energy region of the absorption spectra of both CPEO-[Ru] and LPEO-[Ru] (Scheme S1, Figures S15 and S16 and Table S4). Emission spectra of the two derivatives presented a broad band at 700 nm, whose lifetime was measured to be 262 and 149 ns for CPEO-[Ru] and LPEO-[Ru], respectively. Such features are characteristic of ^{3}MLCT states which are usually emissive in Ru polypyridyl derivatives. The assignment was confirmed by DFT geometry optimization of the lowest-lying triplet of the Ru polypyridyl model complex whose spin density is localized on the Ru atom and the modified bpy ligand (Scheme S1 and Figure S17). Nevertheless, the difference in lifetime between the two structures could be the result of the accessibility of ^{3}LC/IL states. Others have previously demonstrated how the interplay between these two types of excited states is crucial for the photophysical and photochemical features of Ru polypyridyls with extended aromatic ligands.[19, 27] Compared to the cyclic derivative, LPEO-[Ru] could have lower-energy ^{3}LC/IL, laying in the proximity of the emissive ^{3}MLCT, as a result of the higher mobility of the triazole moiety on the functionalized bpy ligand. Such flexibility would ultimately result in a shorter emission lifetime.

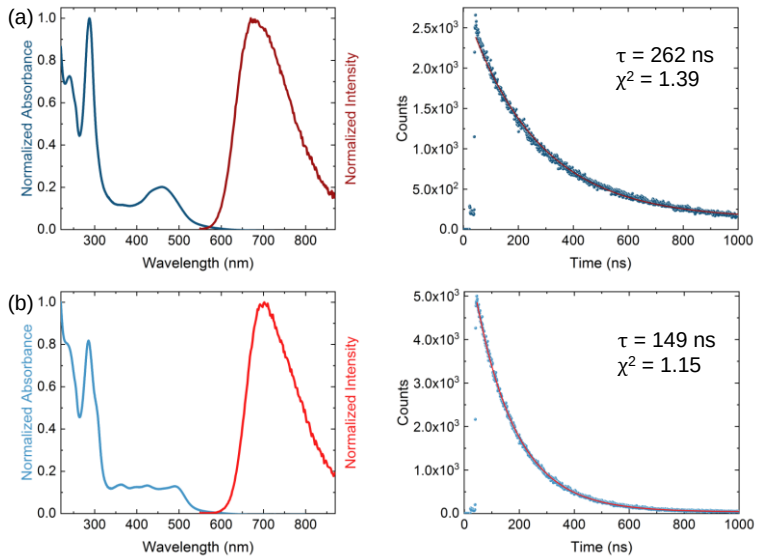

Figure 5. Normalized absorption and normalized emission intensity of (a) CPEO-[Ru] (f1) and (b) LPEO-[Ru] (f1) in water and their radiative decay curves. Emission spectra were obtained using λ_{exc} = 455 nm for CPEO-[Ru] and λ_{exc} = 500 for LPEO-[Ru]. Lifetime measurements were performed using λ_{exc} = 485 nm and λ_{em} = 700 nm.

Next, we investigated the ability of the two PEO-[Ru] topologies to enter cancer cells. To such purpose, MCF7 cells were incubated in the presence of these derivatives for 24 h and subsequently analyzed by flow cytometry upon removing the culture medium and washing with phosphate buffer. Compared to $[Ru(bpy)_3]Cl_2$ (control), cells treated with 140 μM of CPEO-[Ru] and LPEO-[Ru] displayed a marked increase in luminescence that is consistent with a polymer-mediated enhanced internalization of the emissive Ru polypyridyl core (Figure 6, Figure S18 and Table S5). Although more insight is required to gauge whether the photophysics of the complexes is affected by specific cellular compartmentalization and/or aggregation processes, these experiments suggest that CPEO-[Ru] and LPEO-[Ru] are both efficiently internalized by MCF7 cells in a comparable manner. An explanation for such a finding can be reasonably found in the

small MW of PEO-[Ru] complexes (~3 kDa) with no large differences in their size. The radius of gyration (R_g) of LPEO-[Ru] estimated according to $R_{g,\,LPEO} = 0.0215\ M_w^{0.583}$ (R_g in nm and M_w in g/mol),[28] is 2.4 nm and that of CPEO-[Ru] calculated according to $R_{g,\,CPEO} = R_{g,\,LPEO}/\sqrt{2}$,[29] is 1.6 nm. Note that the calculated R_g is a measure of the random coil estimating that the whole polymer chain is exclusively formed by PEO without taking into account the conformational changes that the Ru complex might introduce into the polymer chain. We expect that analogues of CPEO-[Ru] and LPEO-[Ru] with larger sizes could enhance the differences in cell accumulation between the two polymer topologies.

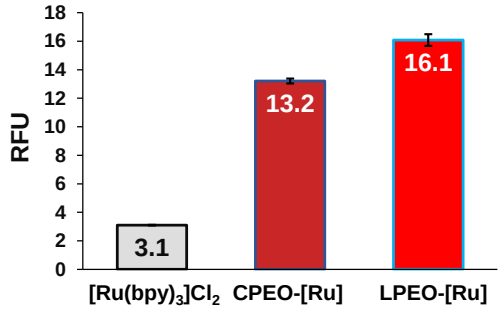

Figure 6. Increase of relative emission intensity of MCF7 cells incubated with $[Ru(bpy)_3]Cl_2$, and with Ru-containing polymers, CPEO-[Ru] and LPEO-[Ru]. Cells incubated with the polymers show a significant increase in relative intensity when compared to those incubated with $[Ru(bpy)_3]Cl_2$. RFU: relative fluorescence units.

In conclusion, CPEO-[Ru] is the first prototype of a Ru polypyridyl cyclic macromolecule featuring a long-lived emission in the red region of the visible spectrum and the capacity of accumulating in MCF7 cancer cells. Future developments in the synthetic design of this family of compounds may afford optically and photochemically active metal architectures of higher MW. With these in hand, new delivery platforms for drugs and

imaging agents can be developed by exploiting the unique biodistribution and pharmacokinetics properties of cyclic polymer topologies.[30]

Supporting Information

Experimental methods, characterization techniques and supporting data including FTIR and NMR spectra of all compounds, calculated mass spectra of polymers, DFT calculation data and flow cytometry analysis.

Acknowledgments

We acknowledge financial support from MCIN/AEI/10.13039/501100011033 and "ERDF A way of making Europe" (PID2021-123438NB-I00), the MICINN (PID2020-117766GB-I00), the Basque Government (Eusko Jaurlaritza grants IT1566-22 and PIBA 2021-1-0034) and Diputación Foral de Gipuzkoa (RED 2021:ID44). DIPC and IMDEA Nanociencia received support from the "Severo Ochoa" Programme for Centres of Excellence in R&D (MINECO, Grants CEX2018-000867-S and CEX2020-001039-S, respectively). L. S. thanks the Spanish Multi-MetDrugs network (RED2018-102471-T) for the fruitful discussion.

Present Addresses

[$]M.A.A.: Faculty of Chemistry, University of the Basque Country UPV/EHU, Paseo Manuel de Lardizabal 3, 20018 Donostia-San Sebastian, Spain

[#]A.T.: University of Palermo, Department of Biological, Chemical and Pharmaceutical Sciences and Technologies, Viale delle Scienze, 90128, Palermo, Italy.

References

1. Liénard, R.; De Winter, J.; Coulembier, O., Cyclic polymers: Advances in their synthesis, properties, and biomedical applications. *J. Polym. Sci.* **2020,** *58* (11), 1481-1502.

2. Haque, F. M.; Grayson, S. M., The synthesis, properties and potential applications of cyclic polymers. *Nat. Chem.* **2020,** *12* (5), 433-444.

3. Ochs, J.; Pagnacco, C. A.; Barroso-Bujans, F., Macrocyclic polymers: Synthesis, purification, properties and applications. *Prog. Polym. Sci.* **2022,** *134*, 101606.

4. Barroso-Bujans, F.; Allgaier, J.; Alegria, A., Poly(ethylene oxide) Melt Intercalation in Graphite Oxide: Sensitivity to Topology, Cyclic versus Linear Chains. *Macromolecules* **2020,** *53* (1), 406-416.

5. Barroso-Bujans, F.; Alegria, A., Kinetic differences in the intercalation of linear and cyclic penta(ethylene oxide)s into graphite oxide leading to separation by topology. *Phys. Chem. Chem. Phys.* **2017,** *19* (28), 18366-18371.

6. Ruiz, D.; Alegria, A.; Barroso-Bujans, F., Isolation of cyclic penta(ethylene oxide) from mixtures with its linear analog by combining selective intercalation into graphite oxide and solvent approaches. *Sep. Purif. Technol.* **2019,** *213*, 142-150.

7. Sawayama, T.; Wang, Y.; Watanabe, T.; Takayanagi, M.; Yamamoto, T.; Hosono, N.; Uemura, T., Metal-Organic Frameworks for Practical Separation of Cyclic and Linear Polymers. *Angew. Chem. Int. Ed.* **2021,** *60* (21), 11830-11834.

8. Nasongkla, N.; Chen, B.; Macaraeg, N.; Fox, M. E.; Fréchet, J. M. J.; Szoka, F. C., Dependence of Pharmacokinetics and Biodistribution on Polymer Architecture: Effect of Cyclic versus Linear Polymers. *J. Am. Chem. Soc.* **2009,** *131* (11), 3842-3843.

9. Chen, B.; Jerger, K.; Fréchet, J. M. J.; Szoka Jr, F. C., The influence of polymer topology on pharmacokinetics: Differences between cyclic and linear PEGylated poly(acrylic acid) comb polymers. *J. Control. Release* **2009,** *140* (3), 203-209.

10. Sun, W.; Li, S.; Häupler, B.; Liu, J.; Jin, S.; Steffen, W.; Schubert, U. S.; Butt, H.-J.; Liang, X.-J.; Wu, S., An Amphiphilic Ruthenium Polymetallodrug for Combined Photodynamic Therapy and Photochemotherapy In Vivo. *Adv. Mater.* **2017,** *29* (6), 1603702.

11. Sun, W.; Parowatkin, M.; Steffen, W.; Butt, H.-J.; Mailänder, V.; Wu, S., Ruthenium-Containing Block Copolymer Assemblies: Red-Light-Responsive Metallopolymers with Tunable Nanostructures for Enhanced Cellular Uptake and Anticancer Phototherapy. *Adv. Healthcare Mater.* **2016,** *5* (4), 467-473.

12. Villemin, E.; Ong, Y. C.; Thomas, C. M.; Gasser, G., Polymer encapsulation of ruthenium complexes for biological and medicinal applications. *Nat. Rev. Chem.* **2019,** *3* (4), 261-282.

13. Moughton, A. O.; O'Reilly, R. K., Using Metallo-Supramolecular Block Copolymers for the Synthesis of Higher Order Nanostructured Assemblies. *Macromol. Rapid Commun.* **2010,** *31* (1), 37-52.

14. Schubert, U. S.; Eschbaumer, C., Macromolecules Containing Bipyridine and Terpyridine Metal Complexes: Towards Metallosupramolecular Polymers. *Angew. Chem., Int. Ed.* **2002,** *41* (16), 2892-2926.

15. Winter, A.; Schubert, U. S., Synthesis and characterization of metallo-supramolecular polymers. *Chem. Soc. Rev.* **2016,** *45* (19), 5311-5357.

16. Zhang, K.; Zha, Y.; Peng, B.; Chen, Y.; Tew, G. N., Metallo-Supramolecular Cyclic Polymers. *J. Am. Chem. Soc.* **2013,** *135* (43), 15994-15997.

17. Hagfeldt, A.; Boschloo, G.; Sun, L.; Kloo, L.; Pettersson, H., Dye-Sensitized Solar Cells. *Chem. Rev.* **2010,** *110* (11), 6595-6663.

18. Prier, C. K.; Rankic, D. A.; MacMillan, D. W. C., Visible Light Photoredox Catalysis with Transition Metal Complexes: Applications in Organic Synthesis. *Chem. Rev.* **2013,** *113* (7), 5322-5363.

19. Monro, S.; Colón, K. L.; Yin, H.; Roque, J., III; Konda, P.; Gujar, S.; Thummel, R. P.; Lilge, L.; Cameron, C. G.; McFarland, S. A., Transition Metal Complexes and Photodynamic Therapy from a Tumor-Centered Approach: Challenges, Opportunities, and Highlights from the Development of TLD1433. *Chem. Rev.* **2019,** *119* (2), 797-828.

20. Heinemann, F.; Karges, J.; Gasser, G., Critical Overview of the Use of Ru(II) Polypyridyl Complexes as Photosensitizers in One-Photon and Two-Photon Photodynamic Therapy. *Acc. Chem. Res.* **2017,** *50* (11), 2727-2736.

21. Gill, M. R.; Thomas, J. A., Ruthenium(ii) polypyridyl complexes and DNA—from structural probes to cellular imaging and therapeutics. *Chem. Soc. Rev.* **2012,** *41* (8), 3179-3192.

22. Laurent, B. A.; Grayson, S. M., Synthetic approaches for the preparation of cyclic polymers. *Chem. Soc. Rev.* **2009,** *38* (8), 2202-2213.

23. Nunes, N.; Popović, I.; Abreu, E.; Maciel, D.; Rodrigues, J.; Soto, J.; Algarra, M.; Petković, M., Detection of Ru potential metallodrug in human urine by MALDI-TOF mass spectrometry: Validation and options to enhance the sensitivity. *Talanta* **2021,** *222*, 121551.

24. Damnjanović, B.; Kamčeva, T.; Petrović, B.; Bugarčić, Ž. D.; Petković, M., Laser desorption and ionization time-of-flightversus matrix-assisted laser desorption and ionization time-of-flight mass spectrometry of Pt(ii) and Ru(iii) metal complexes. *Anal. Methods* **2011,** *3* (2), 400-407.

25. Garino, C.; Terenzi, A.; Barone, G.; Salassa, L., Teaching Inorganic Photophysics and Photochemistry with Three Ruthenium(II) Polypyridyl Complexes: A Computer-Based Exercise. *J. Chem. Educ.* **2016,** *93* (2), 292-298.

26. Karges, J.; Heinemann, F.; Jakubaszek, M.; Maschietto, F.; Subecz, C.; Dotou, M.; Vinck, R.; Blacque, O.; Tharaud, M.; Goud, B.; Viñuelas Zahínos, E.; Spingler, B.; Ciofini, I.; Gasser, G., Rationally Designed Long-Wavelength Absorbing Ru(II) Polypyridyl Complexes as Photosensitizers for Photodynamic Therapy. *J. Am. Chem. Soc.* **2020,** *142* (14), 6578-6587.

27. Kaufmann, M.; Müller, C.; Cullen, A. A.; Brandon, M. P.; Dietzek, B.; Pryce, M. T., Photophysics of Ruthenium(II) Complexes with Thiazole π-Extended Dipyridophenazine Ligands. *Inorg. Chem.* **2021,** *60* (2), 760-773.

28. Devanand, K.; Selser, J. C., Asymptotic behavior and long-range interactions in aqueous solutions of poly(ethylene oxide). *Macromolecules* **1991,** *24* (22), 5943-5947.

29. Rubinstein, M.; Colby, R. H., *Polymer Physics*. Oxford University Press: Oxford, 2003.

30. Chen, C.; Weil, T., Cyclic polymers: synthesis, characteristics, and emerging applications. *Nanoscale Horiz.* **2022,** *7* (10), 1121-1135.